

New Insight into Protein–Ligand Interactions. The Case of the D-Galactose/D-Glucose-Binding Protein from *Escherichia coli*

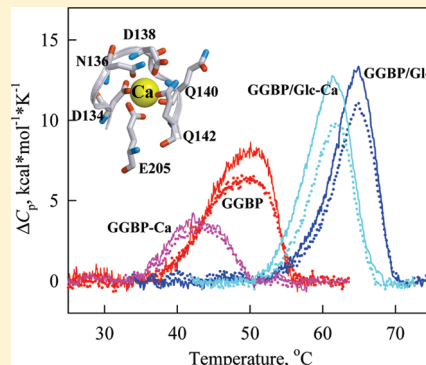
Olga V. Stepanenko,[†] Olesya V. Stepanenko,[†] Olga I. Povarova,[†] Alexander V. Fonin,[†] Irina M. Kuznetsova,[†] Konstantin K. Turoverov,^{*,†} Maria Staiano,^{,‡,§} Antonio Varriale,[‡] and Sabato D'Auria^{*,‡}

[†]Institute of Cytology, Russian Academy of Science, 194064 St. Petersburg, Russia

[‡]CNR, Laboratory for Molecular Sensing, IBP, Naples, Italy

[§]University of Siena, Siena, Italy

ABSTRACT: In this work we have shown that the unfolding-refolding process of the D-galactose/D-glucose-binding protein (GGBP) in the presence of glucose (Glc) induced by the chemical denaturant Gdn-HCl is reversible. In addition, Glc binding does not only stabilize GGBP structure but it also considerably slows down the achievement of the equilibrium between the native protein in GGBP/Glc complex and the unfolded protein. The limiting step of the unfolding-refolding process of the complex GGBP/Glc is the arrangement/de-arrangement of the configuration fit between the protein in the native state and the ligand. The rate of these processes increases/decreases with the increase/decrease of the denaturant concentration. Calcium depletion had a pronounced destabilizing effect on the structure of GGBP but did not affect the stability of GGBP/Glc complex. Unfolding of GGBP/Ca complex is reversible. Only incubation of the unfolded protein at high temperature leads to an irreversible process due to the aggregation of the protein. The amount of protein aggregation is determined by the protein concentration, the temperature and the duration of the incubation.



INTRODUCTION

One of the most intriguing questions of modern molecular and cell biology is how a globular protein folds into a unique, compact, highly organized and functionally active state.^{1–8} In the past decade, our knowledge about protein folding into the native state and even the notion of native state itself have undergone considerable changes. At the turn of the century, publications appeared that showed that polypeptide chains of many proteins could not in principle fold into a compact globular state. Although these proteins are intrinsically disordered, they are functionally active and notably are native.^{8–10} These proteins form a compact globular state only upon interactions with their specific partners such as low molecular weight ligands, other protein molecules, or nucleic acids. As a consequence, understanding the effects on proteins of binding with ligands is of great interest.

Two-domain ligand-binding proteins of the bacterial periplasm (PBP) can be convenient models to investigate the role of the ligand in the folding and in the stabilization of proteins in the native state. These bacterial proteins are primary receptors for a large number of compounds (for example, carbohydrates, amino acids, anions, metal ions, dipeptides and oligo-peptides), and they are involved in the active transport of the soluble molecules inside the bacterial cell. In some cases, these proteins participate in chemotaxis toward different substances^{11–13} and in bacterial quorum sensing.^{11,14} The molecular weight of ligand-binding proteins ranges from 22 to 59 kDa. Despite significant differences

in their amino acid sequences, all ligand-binding proteins share the same structural topology of the polypeptide chain. All of them display an α/β type of secondary structure that is organized at the tertiary level into two domains linked by what is commonly referred to as a hinge region. The active site for substrate binding is located in the cleft between the two domains. It becomes partially closed upon binding of the ligand. Protein dissociation constants vary from $0.1 \mu\text{M}$ for the binding of amino acids to $1 \mu\text{M}$ for the binding of sugars.

In this work, we studied the unfolding–refolding mechanisms induced by guanidine hydrochloride (Gdn-HCl) or heating on the D-galactose/D-glucose-binding protein (GGBP) from *Escherichia coli* in its open and closed forms, i.e., when it is in the sugar-free state and when it is in a complex with D-glucose (GGBP/Glc). An additional task of the work was to study the role of calcium on the stability of the protein.^{15,16}

The study of the structure and stability features of GGBP in its open and closed forms is of high interest in view of the possibility of using GGBP to construct a biosensor system to monitor glucose levels in the blood of diabetic patients.^{17,18} GGBP could be used as a sensing element for glucose detection because binding of the ligand to GGBP results in a significant conformational change of the protein structure.^{19–21}

Received: October 5, 2010

Revised: December 20, 2010

Published: February 18, 2011

■ MATERIALS AND METHODS

Materials. GGBP from *E. coli* was obtained and purified as described previously.²⁰ The samples of D-glucose (Sigma, USA) and Gdn-HCl (Nacalai Tesque, Japan) were used without purification. The concentration of Gdn-HCl in solution was determined by a refractometric method²² using an Abbe refractometer (LOMO, Russia). The protein concentration was 0.1–0.65 mg/mL. The GGBP/Glc complex was formed by adding D-glucose to a final concentration of 10 mM. Calcium-ion-depleted forms of the protein were obtained by adding EDTA (Fluka, Sweden) to a final concentration of 0.18 mM. All experiments were carried out in 10 mM Na-phosphate buffered solution at pH 8.0.

Analysis of Protein 3D Structure. A comparative analysis of the microenvironment peculiarities of tryptophan and tyrosine residue localization in the structure of GGBP and its complex GGBP/Glc was done on the basis of PDB data²³ using the 2FW0.ent¹⁶ and 2GBP.ent¹⁵ files, respectively. The analysis of the microenvironment properties of tryptophan and tyrosine residue localization in the protein was performed as described previously.^{24–26}

Fluorescence Measurements. The fluorescence experiments were carried out using a Cary Eclipse spectrophotofluorimeter (Varian, Australia) with microcells (10 × 10 mm; Varian, Australia). Fluorescence anisotropy and fluorescence lifetime were measured using a homemade spectrophotofluorimeter with steady-state and time-resolved excitation²⁷ using microcells (101.016-QS 5 × 5 mm; Hellma, Germany). The excitation wavelengths for fluorescence spectra were 297 and 280 nm. The position and form of fluorescence spectra were characterized by the parameter $A = I_{320}/I_{365}$, where I_{320} and I_{365} are fluorescence intensities measured at the emission wavelengths of 320 and 365 nm, respectively.²⁵ The values of parameter A and the fluorescence spectra were corrected by the instrument's spectral sensitivity. The contribution of tyrosine residues was characterized by the value $\Delta_{\lambda,Tyr} = (I_{\lambda}/I_{365})_{280} - (I_{\lambda}/I_{365})_{297}$.

The equilibrium dependencies of different fluorescence characteristics for GGBP in the presence of different Gdn-HCl concentrations were recorded after protein incubation in solutions of an appropriate denaturant concentration at 4 °C overnight if not specified. The measurements were performed at 23 °C. For a more detailed analysis of the protein unfolding process and to determine the number of intermediate states appearing on the pathway from the native to the unfolded protein, we used a method of parametric representation of the two independent extensive parameters of the system.^{28–31} The thermodynamic characteristics of protein stability were calculated according to the standard scheme.³² The decay fluorescence curves were analyzed using the multiexponential approach. The fitting routine was accomplished using the nonlinear least-squares method with a Marquardt minimization algorithm.³³ A solution of *p*-terphenyl in ethanol and a water solution of *N*-acetyl tryptophan amide were used as standards.³³

Far-UV Circular Dichroism Measurements. Circular dichroism (CD) spectra were obtained using a Jasco-810 spectropolarimeter (Jasco, Japan). CD spectra were recorded in a 1-mm path length cell from 260 to 190 nm with a step size of 0.1 nm. For all spectra, an average of three scans were obtained. CD spectra of the appropriate buffer solution were recorded and subtracted from the protein spectra.

DSC Measurements. Differential scanning calorimetry (DSC) experiments were performed using a DASM-4 differential

scanning microcalorimeter (“Biopribor”, Pushchino, Russia) as described earlier.^{34–36} Protein samples (0.65 mg/mL) were heated at a constant rate of 1 K/min at a constant pressure of 2.4 atm. The reversibility of the thermal transitions was assessed by reheating the sample immediately after the cooling step from the previous scan. The thermal transition curves were baseline corrected by subtracting a scan of only buffer in both cells. The protein's excess heat capacity (C_p) was calculated as described by Privalov and Potekhin.³⁷ The temperature dependence of the excess heat capacity was analyzed using Origin software (Micro-Cal Inc., Northampton, MA). The thermal stability of the proteins was described by the temperature of the maximum of thermal transition (T_m), and calorimetric enthalpy (ΔH_{cal}) was calculated as the area under the excess heat capacity curve.

■ RESULTS AND DISCUSSION

GGBP has the two-domains structure, typical of PBPs (Figure 1, a and b). The N-terminal and C-terminal domains each consist of a six β-strand core surrounded by two or three α-helices on different sides of the core. The ligand-binding site is located in a deep cleft between the two domains (Figure 1, c).¹³ A pocket for sugar binding is formed by two aromatic amino acids, Phe 16 and Trp 183, which belong to the protein N- and C-terminal domains, respectively. At the binding site eight additional amino acids and one water molecule create a strong network of 13 hydrogen bonds with all the hydroxyls and oxygen atoms of the D-glucose ring.¹⁵ The Ca-binding center is located in the loop of the protein's C-terminal domain (residues 134–142), and its structure resembles the “EF-hand” motif, typical of intracellular Ca-binding proteins (Figure 1, d).^{15,16} The calcium ion forms coordination bonds with oxygen atoms and with the Glu 205 residue (Figure 1, d).

The CD spectrum of GGBP (Figure 2) is typical for proteins with a high content of α-helical regions in their secondary structure. The CD spectrum undergoes almost no change upon D-glucose binding, which indicates that the protein secondary structure changes insignificantly in the transition to the closed form.

The intrinsic fluorescence spectrum of GGBP is red-shifted ($\lambda_{em} = 345–346$ nm at $\lambda_{ex} = 297$ nm, Figure 3). The analysis of the peculiarities of the location and characteristics of the microenvironments of the tryptophan and tyrosine residues in GGBP performed as described previously^{25–27} allowed us to explain the position of the GGBP fluorescence spectrum.

Although there are seven tyrosine residues in GGBP, their contribution to the bulk fluorescence of the protein is very low. Such low fluorescence contribution can be explained, on the basis of the localization of tyrosine and tryptophan residues in the protein structure, by effective tyrosine–tyrosine and tyrosine–tryptophan nonradiative energy transfer phenomena. Tryptophan residues are located in α-helices (Trp 127 and Trp 195) and in unstructured regions of the polypeptide chain (Trp 133, Trp 183, and Trp 284). All of them have a rather polar microenvironment, which is the reason why we observe such a long-wavelength shifted fluorescence spectrum for GGBP. These data are in good agreement with previous data,³⁸ where the maximum of the GGBP fluorescent spectrum was recorded at 344 nm ($\lambda_{ex} = 295$ nm). Only one of the five tryptophan residues of GGBP (Trp 284) is located at the N-terminal domain, whereas all the other Trp residues (Trp 127, Trp 133, Trp 183, and Trp 195) are part of the protein C-terminal domain. One of these

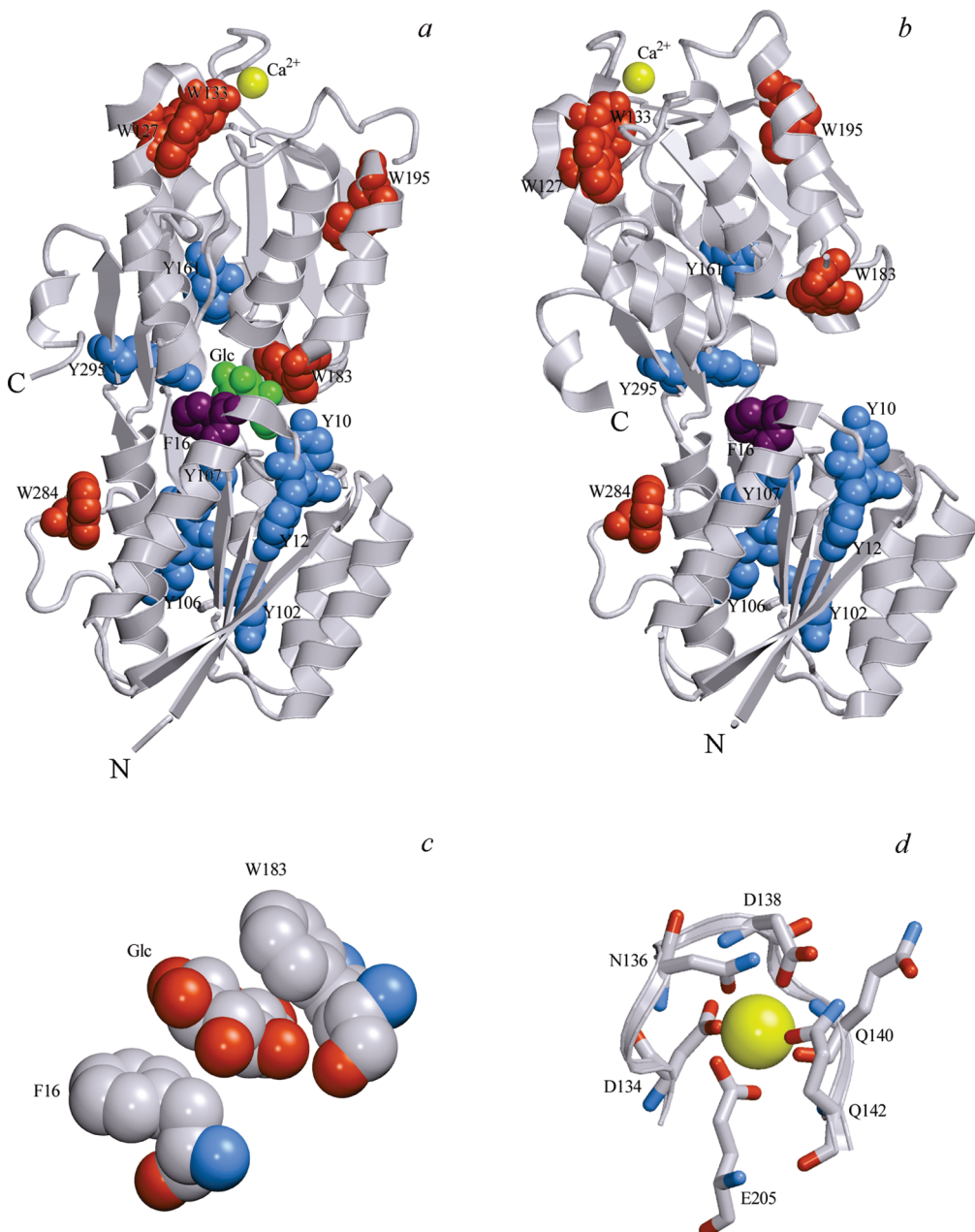


Figure 1. 3D structure of D-galactose/D-glucose-binding protein (GGBP) and its complex with D-glucose (GGBP/Glc). Localization of tryptophan (red) and tyrosine (blue) residues in the structures of GGBP/Glc and GGBP is presented in panels (a) and (b), respectively. The Ca ion (yellow) and a bound molecule of D-glucose (green) are presented as van der Waals spheres. Localization of D-glucose between the aromatic rings of Phe 16 and Trp 183, which are included in the sugar-binding center, is given in panel (c). The structure of the calcium-binding center is shown in panel (d). Residues coordinating the calcium ion are depicted. Carbon, nitrogen, and oxygen are gray, blue, and red, respectively. The figure was created on the basis of PDB²³ data with the files 2GBP.ent¹⁵ and 2FWO.ent¹⁶ using the graphical software VMD⁴³ and Raster 3D.⁴⁴

residues, Trp 183, is oriented toward the innermost region of the cleft that serves as a ligand binding site. This tryptophan residue and the Phe 16 residue of the protein N-terminal domain participate in the binding of the sugar by forming an aromatic pocket. The sugar molecule incorporates between the benzene ring of Phe 16 and the indole ring of Trp 183 (Figure 1, c). D-Glucose binding is accompanied by significant changes of the relative position of the two domains, but the structure of the protein domains remains practically unchanged. Nonetheless, the analysis of the protein structure revealed small changes in the microenvironment of Trp 183 that could lead to a limited blue

shift of the fluorescence spectrum. These changes were not recorded previously.³⁸ In this report, we have recorded small (1–2 nm) but reliable blue shifts of the fluorescence spectrum upon glucose binding. Not only the shape and the position of the fluorescence spectrum of GGBP change almost insignificantly upon ligand binding but also the anisotropy value and the lifetime are substantially the same in the ligand-free and in the ligand-bound states (Table 1).

We also analyzed by far-UV CD the open and closed forms of the holo protein in the absence (GGBP) and in the presence of glucose (GGBP/Glc) as well as the calcium-depleted GGBP

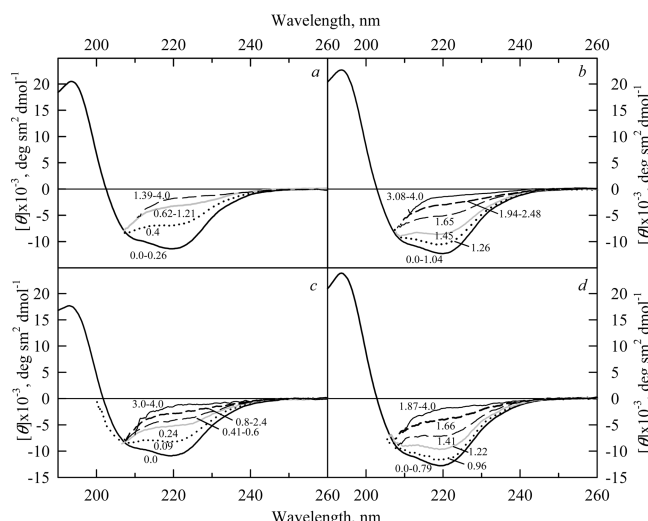


Figure 2. Far-UV CD spectra of GGBP (a) and GGBP/Glc (b) and their calcium-depleted forms GGBP-Ca (c) and GGBP/Glc-Ca (d) recorded for protein samples containing different amounts of Gdn-HCl. The values on the curves are Gdn-HCl concentrations.

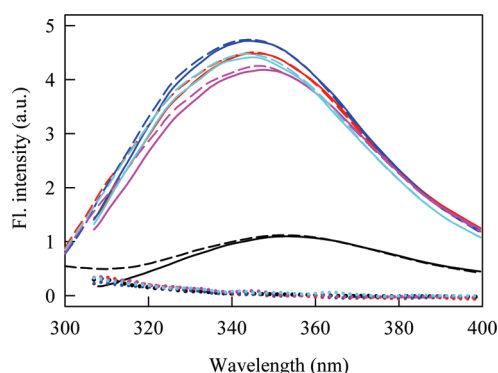


Figure 3. Fluorescence spectra of GGBP (red) and GGBP/Glc (blue) and their calcium-depleted forms GGBP-Ca (pink) and GGBP/Glc-Ca (light blue). The fluorescence spectrum of GGBP in its unfolded state (in the presence of 3 M of Gdn-HCl) is presented in black. Excitation wavelengths are 297 nm (solid lines) and 280 nm (dashed lines). The contribution of tyrosine residues is also presented.

(GGBP-Ca) in the absence and in the presence of glucose (GGBP/Glc-Ca). We found that calcium depletion did not result in noticeable changes of the far-UV CD spectra of GGBP and GGBP/Glc (Figure 2). This result indicates that the binding/depletion of calcium is accompanied by small alterations of the protein's secondary structure content both in the open and in the closed form. In our previous work on GGBP performed by FTIR spectroscopy,³⁹ we showed the presence of slight changes of the α -helical content of GGBP after calcium depletion.³⁹ In this work, a minimal decrease of GGBP fluorescence intensity and a slight red shift of 1–2 nm of GGBP fluorescence spectrum position were observed during calcium depletion in the open and closed GGBP forms (Figure 3). The different forms of GGBP with respect to the position of the maximum of their fluorescence spectra can be represented as follows: GGBP/Glc < GGBP/Glc-Ca \approx GGBP < GGBP-Ca. This suggests that calcium removal results in a partial loosening

of GGBP protein tertiary structure. Nonetheless, GGBP open form undergoes the largest structural variation upon calcium depletion. After calcium depletion, the compactness of the GGBP/Glc (closed form) is similar to that of holo GGBP. These results point out the stabilizing effect of calcium in the GGBP open form.

Gdn-HCl-Induced Unfolding–refolding of GGBP in the Open and Closed Forms. The Role of Calcium in These Processes. The effect of different concentrations of Gdn-HCl on GGBP at equilibrium or quasi-equilibrium both in the absence and in the presence of glucose were monitored by using several spectroscopic strategies such as fixed wavelength monitoring of fluorescence intensity, or the use of parameter A values, or fluorescence anisotropy, or circular dichroism values at 222 nm. In all cases, we obtained sigmoid shaped curves (Figure 4) suggesting a one-step unfolding process for both GGBP and GGBP/Glc. A one-step process is also supported by the linear dependence of the fluorescence intensity values recorded at 320 nm and at 365 nm (Figure 5). At the same time, the equilibrium dependencies of different structural probes on Gdn-HCl concentration can be sigmoid, and parametric dependencies between fluorescence intensities at different emission wavelengths can be linear even if concealed intermediate states exist but their properties are intermediate with respect to that of the native and unfolded states of the protein. Similar results were described for the Gdn-HCl-induced denaturation of bovine carbonic anhydrase II.⁴⁰ The intermediate state like a molten globule state of carbonic anhydrase II was revealed only by significant changes of the ANS (ammonium salt of 8-anilinonaphthalene-1-sulfonic acid) fluorescence intensity. Therefore, we recorded the dependence of ANS fluorescence intensity of GGBP on the concentration of Gdn-HCl in the range between 0.0 and 4.0 M Gdn-HCl. This experiment proved the absence of a masked intermediate state during the Gdn-HCl-induced unfolding of GGBP. Furthermore, we recorded the kinetics of unfolding and refolding processes for GGBP (Figure 6). The obtained experimental curves fit with a monoexponential model, indicating a one-stage transition process.

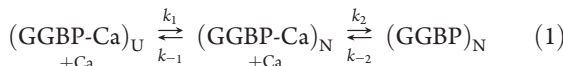
While studying the effect of calcium depletion on the denaturation of the protein, we noticed that the values of the fluorescence characteristics and ellipticity at 222 nm were dramatically different between GGBP and GGBP-Ca even at low denaturant concentrations (Figure 4). However, the equilibrium dependencies of different structural probes of the GGBP closed form without calcium practically coincide with those of GGBP/Glc (Figure 4). These results indicate that the role of calcium consists of maintaining the native structure of GGBP in the open form.

The fluorescence spectrum of GGBP in 3.0–4.0 M Gdn-HCl has an emission maximum at 353 nm (Figure 3). The fluorescence intensity and the lifetime values of the unfolded protein are significantly lower than those of GGBP in the native state (Figure 3, Table 1). These differences can be explained by the quenching action of the solvent (water molecules) on the protein tryptophan residues that become accessible to the solvent during the transition of the protein structure to the unfolded state. A decrease of GGBP tryptophan intensity fluorescence during Gdn-HCl-induced protein unfolding is accompanied by the reduction of the lifetime, which is apparently determined by the increased dynamic quenching of the tryptophan fluorescence by solvent molecules.⁴¹

Table 1. Features of Intrinsic Fluorescence of GGBP and GGBP/Glc in the Native State and Unfolded State

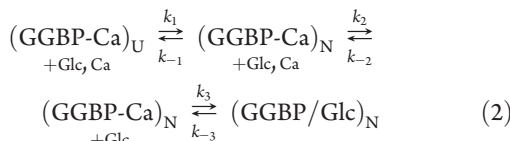
parameter	Gdn-HCl concentration, M	parameter A ($\lambda_{\text{ex}} = 297 \text{ nm}$)	$r (\lambda_{\text{ex}} = 297 \text{ nm}, \lambda_{\text{em}} = 365 \text{ nm})$	$\langle \tau \rangle, \text{ns} (\lambda_{\text{ex}} = 297 \text{ nm}, \lambda_{\text{em}} = 350 \text{ nm})$
Native Protein				
GGBP		0.87	0.14	6.15
GGBP/Glc		0.88	0.15	6.22
Protein in Unfolded State				
GGBP	3.0 M	0.46	0.06	2.60
GGBP/Glc	3.0 M	0.45	0.06	2.75
Protein Renatured from the Unfolded State (2.8 M Gdn-HCl)				
GGBP	0.3	0.83	0.13	6.03
GGBP in the presence of 10 mM Glc	0.3	0.86	0.15	5.81

Processes of GGBP unfolding–refolding meet the following kinetics scheme



Stationary curves of GGBP unfolding–refolding processes after protein incubation in the Gdn-HCl solutions of appropriate concentrations for 24 h coincide (Figure 7, a). In reality, the equilibration is reached even faster. It suggests that the process is reversible and that Ca binding with $(GGBP\text{-Ca})_N$ is a fast process. Apparently, the limiting stage of protein folding is the formation of protein native state. Anyhow, the curve of GGBP unfolding–refolding is equilibrium and can be used for determination of the difference between free energies of protein in native and unfolded states (ΔG_2 , Figure 7, b).

The process of complex GGBP/Glc unfolding–refolding is determined by the following kinetic scheme



In our work, we measured the curve of the unfolding process of GGBP/Glc after 24 h of incubation in the Gdn-HCl solutions of appropriate concentrations (Figure 7, a, blue dashed curve). It was shifted to the larger concentrations of Gdn-HCl in comparison with the GGBP unfolding–refolding curve. The GGBP glucose binding constant is known to be very large¹⁵ (about $1.0 \mu\text{M}^{-1}$). So, we supposed that GGBP/Glc complex formation from GGBP and Glc would not be a limiting stage of this process. Nonetheless, the experiments on protein refolding showed that complex renaturation after 24 h incubation in the solutions of appropriate concentrations of Gdn-HCl (Figure 7, a, blue closed squares) does not coincide with the denaturing curve but is much closer to the curve corresponding to GGBP unfolding–refolding (Figure 7, a, red curve). This result was rather unexpected because it can be so only if the process of GGBP complex formation with Glc is a limiting stage in GGBP/Glc formation from $(GGBP)_U$ in the presence of the excess of Glc and Ca. This means that the curves of denaturation after 24 h of incubation in the appropriate concentrations of Gdn-HCl were not equilibrium curves. We have shown that equilibrium curves of unfolding and refolding coinciding to each other can be obtained after 10 days of incubation in the Gdn-HCl of appropriate concentration

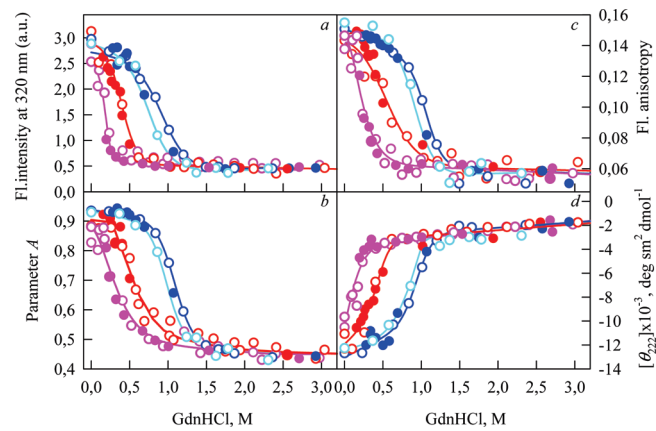


Figure 4. Conformational changes of GGBP and GGBP-Ca (red and pink circles, respectively) and GGBP/Glc and GGBP/Glc-Ca (blue and light blue circles, respectively) induced by Gdn-HCl. (a) Changes in fluorescence intensity recorded at 320 nm. (b) Changes of parameter A. (c) Changes of fluorescence anisotropy for an excitation wavelength of 297 nm. (d) Changes in ellipticity at 222 nm. Open symbols indicate unfolding whereas closed symbols represent refolding. In the case of GGBP, GGBP-Ca, and GGBP/Glc, equilibrium dependencies of different structural probes measured on the pathway of protein renaturation from the unfolded state coincide with the corresponding dependencies obtained on the pathway of protein denaturation. In the case of GGBP/Glc-Ca, the renaturation process does not come to equilibrium even after 10 days of incubation, but renaturation curves tend to close denaturation curves.

(Figures 4 and 7, a, blue solid curve). The curve of the GGBP/Glc-Ca unfolding reached equilibrium after 10 days of incubation. At the same time, renaturation of GGBP/Glc-Ca takes even longer time (data not shown).

The repeated denaturation of protein after renaturation in the presence of Glc and without it (Figure 8) shows that protein in the presence of Glc unfolds much slower in comparison with protein. This suggests that renaturation leads to ligand rebounding.

In conclusion, we showed that dependencies of the molecule fractions in the unfolded $(GGBP)_U$ and native complex $(GGBP\text{/Glc})_N$ states (in the presence of the excess concentrations of Glc and Ca) upon Gdn-HCl concentration became equilibrium after 10 days of sample incubation in the solution of appropriate denaturant concentration. Before equilibrium is established for a long time there is the excess concentration (in comparison with equilibrium) of complex $(GGBP\text{/Glc})_N$ on the pathway of unfolding or unfolded protein $(GGBP)_U$ on the pathway of

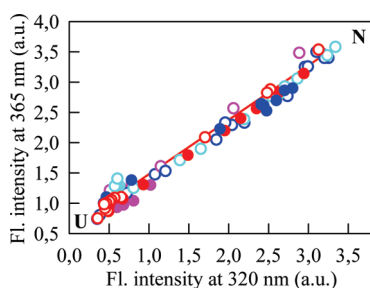


Figure 5. Parametric dependencies between fluorescence intensities recorded at 320 and 365 nm in the unfolding and refolding processes of GGBP and GGBP-Ca (red and pink circles, respectively) and GGBP/Glc and GGBP/Glc-Ca (blue and light blue circles, respectively) induced by Gdn-HCl. The parameter is Gdn-HCl concentration. The excitation wavelength was 297 nm. Open symbols indicate unfolding, whereas closed symbols represent refolding.

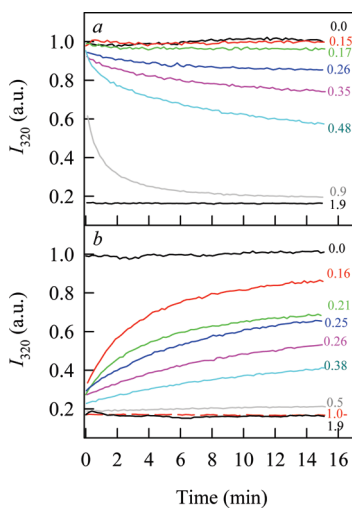


Figure 6. Kinetics of tryptophan fluorescence intensity changes accompanying unfolding (a) and refolding (b) of GGBP. Kinetic curves for protein have been normalized to its fluorescence intensity in the native state. The values on the curves represent the values of Gdn-HCl concentrations. $\lambda_{\text{ex}} = 297$ nm.

renaturation. It is so because the activation barrier must be overcome in both cases. On the pathway of unfolding, the elementary act of complex dissociation does not lead to the disturbance of configuration fit of interacting molecules of GGBP and Glc, and consequently the probability of the inverse reaction is high. Contrary, on the pathway of refolding it is so because for complex formation not only the formation of native molecule ($(\text{GGBP})_N$) but also the appearance of configuration fit of ($(\text{GGBP})_N$) molecule and Glc is needed.

The dependences on Gdn-HCl concentration of the fraction of molecules in the native state for GGBP, GGBP/Glc, and their calcium-depleted forms were calculated from the fluorescence intensity and the ellipticity at 222 nm (Figure 9). For all protein forms (GGBP, GGBP/Glc, GGBP-Ca, and GGBP/Glc-Ca), the curves derived from measures of two different structural probes are substantially identical. This indicates that, during Gdn-HCl-induced GGBP unfolding, the secondary and tertiary structures of the protein are lost simultaneously. The equilibrium dependence on Gdn-HCl concentration of the fluorescence intensity at a fixed registration wavelength for GGBP and GGBP/Glc, and of

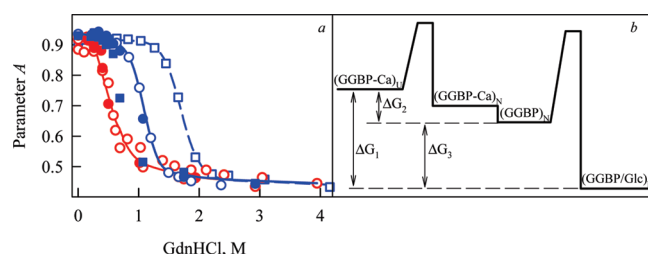


Figure 7. Gdn-HCl-induced conformational transitions of GGBP and GGBP/Glc. (a) The change of parameter $A = I_{320}/I_{365}$. Unfolding curves were measured for GGBP after incubation in solutions of an appropriate denaturant concentration at 4 °C during 24 h (red solid line and red open circles) and for GGBP/Glc after incubation during 24 h (blue dashed line and blue open squares) and 10 days (blue solid line and blue open circles). Data characterizing protein renaturation from the unfolded state were measured after incubation in solutions of an appropriate denaturant concentration at 4 °C during 24 h for GGBP (red closed circles) and during 24 h (blue closed squares) and 10 days for GGBP/Glc (blue closed circles). $\lambda_{\text{ex}} = 297$ nm. (b) Energy scheme characterizing the GGBP and GGBP/Glc unfolding–refolding processes.

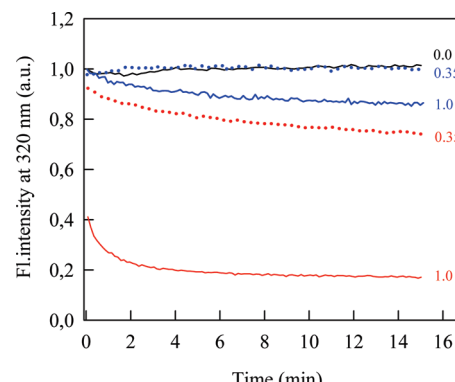


Figure 8. Kinetics of tryptophan fluorescence changes accompanying unfolding of GGBP (curves in red) and GGBP/Glc (curves in blue). Measurements were performed on the protein and on its complex with glucose which had previously been subjected to an unfolding–refolding cycle. The values on the curves represent the values of Gdn-HCl concentrations. $\lambda_{\text{ex}} = 297$ nm.

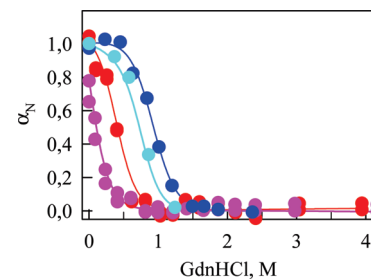


Figure 9. Fraction of native molecules (α_N) of GGBP and GGBP-Ca (red and pink circles, respectively) and GGBP/Glc and GGBP/Glc-Ca (blue and light blue circles) at different concentrations of Gdn-HCl. The fraction of native molecules was calculated on the basis of the dependences of tryptophan fluorescence recorded at 320 and 365 nm and the ellipticity at 222 nm.

their calcium-depleted forms, GGBP-Ca and GGBP/Glc-Ca were used to evaluate the free energy differences between the protein in its native and in its unfolded state, ΔG^0 (Table 2). The ΔG^0 value of GGBP/Glc (3.37 ± 1.07 kcal mol $^{-1}$) is almost twice as high as that of GGBP (1.92 ± 0.90 kcal mol $^{-1}$). This finding indicates that the binding of D-glucose results, as expected, in a significant stabilization of the GGBP structure. The ΔG^0 value of the GGBP open form depleted of calcium can not be defined accurately because it was impossible to estimate the fluorescence intensity of the native state (Figures 4 and 9). However, it is obvious that this protein form is very unstable. In addition, the ΔG^0 value of the GGBP closed form after calcium removal is practically unchanged. These comparisons support the stabilizing role of calcium on the structure of GGBP in the open form, unbound to glucose.

Table 2. Thermodynamic Parameters of GGBP and GGBP/Glc and Their Calcium-Depleted Forms Determined on the Basis of a Gdn-HCl-Induced Unfolding Process

	GGBP-Ca	GGBP	GGBP/Glc-Ca	GGBP/Glc
m , kcal mol $^{-1}$ M $^{-1}$	6.17 ± 3.28	5.29 ± 1.42	4.17 ± 1.03	3.60 ± 0.88
$D_{50\%}$, M	0.07 ± 0.12	0.36 ± 0.10	0.76 ± 0.06	0.93 ± 0.03
ΔG^0 (23 °C), kcal mol $^{-1}$	0.42 ± 0.95	1.92 ± 0.9	3.18 ± 1.05	3.37 ± 1.07

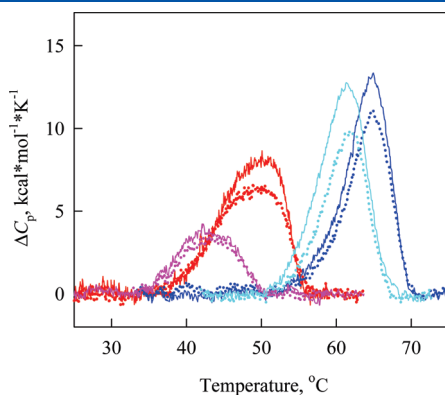


Figure 10. Temperature dependencies of the excess heat capacity of GGBP and GGBP-Ca (red and pink, respectively) as well as GGBP/Glc and GGBP/Glc-Ca (blue and light blue, respectively). Protein concentration was 0.65 mg/mL. Two sequential scans (solid and dotted lines, respectively) are shown to characterize the reversibility of the thermal transitions.

Heat-Induced Denaturation of GGBP and GGBP/Glc. The thermostability of GGBP in its open and closed forms has already been studied by several methods.^{38,39,42} For example, DSC (differential scanning calorimetry) data showed the reversibility of the heat-induced denaturation of GGBP and GGBP/Glc,⁴² but different experiments indicated the formation of protein aggregates upon thermal unfolding.^{38,39} This discrepancy encouraged us to undertake additional investigations on the thermal denaturation of GGBP using DSC. The protein calorimetric traces were obtained in the presence and absence of the ligands, D-glucose and calcium (Figure 10 and Table 3). The temperature of the maximum of thermal transition T_m of GGBP was 50.5 °C. Sugar binding results in a significant shift (13.9 °C) of the GGBP/Glc thermal transition to a higher temperature ($T_m = 64.4$ °C). In addition, compared to that of GGBP, the thermal transition curve of GGBP/Glc is more pronounced and tight. These results imply an increased cooperativity in GGBP/Glc thermal unfolding and a predictable stabilizing action of D-glucose on the protein structure. Calcium removal from GGBP in the open form results in a more pronounced shift of the thermal transition as compared to that of GGBP in the closed form. The temperatures of the maximum of thermal transition of calcium-depleted GGBP and GGBP/Glc are equal to 42.7 and 61.5 °C, respectively. These temperatures are 7.8 and 2.9 °C lower than the corresponding temperatures of calcium containing GGBP and GGBP/Glc (Figure 10 and Table 3). These results allowed us to confirm that calcium has a stabilizing effect on the protein structure of the open form of GGBP, against different denaturing agents. Previous tryptophan fluorescence, far-UV CD, and IR experiments also revealed a significant destabilization of GGBP in the open form when calcium was removed, as it resulted in a 10 °C decrease of the GGBP-Ca melting temperature and in a less cooperative thermal transition.^{39,41} Moreover, the experiments showed that the thermostability of GGBP/Glc-Ca is higher than that of GGBP-Ca. We corroborated these data by DSC studies of GGBP-Ca and GGBP/Glc-Ca, and the results indicate that calcium overcomes the destabilization of the protein structure when it is converted to the GGBP open form. The heat-induced denaturation of GGBP is reversible both in the presence and in the absence of ligands. Cooling of the protein solution to room temperature leads to the recovery of parameter A and of the fluorescence anisotropy back to the levels of the native protein (Table 3). Heating the protein to a temperature that exceeds the end of the thermal transition leads to an irreversible thermal unfolding as indicated by a lack of complete coincidence between calorimetric traces after reheating (Figure 10) and by a decrease of the GGBP fluorescence

Table 3. Calorimetric Parameters Obtained from DSC Data for Thermal Transitions of GGBP, GGBP/Glc, and Their Calcium-Depleted Forms^a

protein sample	T_m , °C	ΔH_{cal} , kcal/mol	parameter A ($\lambda_{ex} = 297$ nm)		r ($\lambda_{ex} = 297$ nm, $\lambda_{em} = 365$ nm)	
			before	after	before	after
GGBP	50.5	95	0.87	0.85	0.16	0.16
GGBP/Glc	64.4	92	0.85	0.84	0.16	0.16
GGBP-Ca	42.7	36	0.89	0.86	0.15	0.15
GGBP/Glc-Ca	61.5	100	0.86	0.83	0.16	0.15

^a The parameters were extracted from Figure 10. The errors of the given values of transition temperature (T_m) did not exceed ± 0.2 °C. The relative errors of the given values of calorimetric enthalpy, ΔH_{cal} , did not exceed $\pm 10\%$. The intrinsic fluorescence characteristics of the protein before and after thermal denaturation are shown.

intensity and far- and near-UV CD values. We found that as the final temperature reached in protein heating increases the reversibility of the denaturation of GGBP decreases. We suggest that the heat-induced denaturation of GGBP is complicated by protein aggregation both in the presence and in the absence of ligands. These processes occur even if the heating of the protein is performed in the presence of Gdn-HCl (data not shown). The amount of aggregated protein is influenced by several factors such as protein concentration, the temperature of heating, and the duration of protein incubation at high temperature.

CONCLUSIONS

All experimental data obtained by intrinsic protein fluorescence and far-UV CD as well as the parametric representation of fluorescence data, which is an effective tool for the detection of hidden protein intermediate states, indicate that the process of GGBP and GGBP/Glc unfolding induced by Gdn-HCl is a one-step reversible process. ANS fluorescence measurements also indicate the absence of intermediate states. Both the open and closed forms of GGBP unfold rather cooperatively. As was expected, D-glucose binding stabilizes the protein against the denaturing action of Gdn-HCl. Furthermore, it considerably slows down the achievement of the equilibrium between the native protein in GGBP/Glc complex and the unfolded protein. The limiting step of the unfolding-refolding process of the complex GGBP/Glc is the arrangement/dearrangement of the configuration fit between the protein in the native state and the ligand. The rate of these processes increases/decreases with the increase/decrease of denaturant concentration. The significant role of calcium in stabilizing the native structure of GGBP in the open form was shown. The heat-induced denaturation of GGBP in the presence and absence of ligands was also described as a reversible process, which is complicated by protein aggregation during incubation of the protein at high temperatures. The degree of aggregation is influenced by protein concentration, the heating temperature, and the duration of protein incubation at high temperatures.

AUTHOR INFORMATION

Corresponding Author

*Dr. Konstantin K. Turoverov. Tel.: 7(812) 2971957. Fax: 7(812) 2970341. E-mail: kkt@mail.cytspb.rssi.ru. Dr. Sabato D'Auria. Tel.: +39-0816132250. Fax: +39-0816132277. E-mail: s.dauria@ibp.cnr.it.

ACKNOWLEDGMENT

This project was supported by NATO grant CLG.983088, contracts with FASI (02.512.11.2277 and 02.740.11.5141) and FAE (P1198), Program MCB RAS, and a grant from the president of RF (MK-1181.2010.4).

ABBREVIATIONS

ANS, ammonium salt of 8-anilinonaphthalene-1-sulfonic acid; CD, circular dichroism; DSC, differential scanning calorimetry; GGBP, D-galactose/D-glucose-binding protein from *Escherichia coli*; GGBP/Glc, complex of GGBP with D-glucose; GGBP-Ca and GGBP/Glc-Ca, calcium-depleted form of GGBP and GGBP/Glc, respectively; Gdn-HCl, guanidine hydrochloride; UV, ultraviolet

REFERENCES

- (1) Jahn, T. R.; Radford, S. E. *FEBS J.* **2005**, *272*, 5962–70.
- (2) Jahn, T. R.; Radford, S. E. *Arch. Biochem. Biophys.* **2008**, *469*, 100–17.
- (3) Lindorff-Larsen, K.; Rogen, P.; Paci, E.; Vendruscolo, M.; Dobson, C. M. *Trends Biochem. Sci.* **2005**, *30*, 13–9.
- (4) Brockwell, D. J.; Radford, S. E. *Curr. Opin. Struct. Biol.* **2007**, *17*, 30–7.
- (5) Finkelstein, A. V.; Ivankov, D. N.; Garbuzynskiy, S. O.; Galzitskaya, O. V. *Curr. Protein Pept. Sci.* **2007**, *8*, 521–36.
- (6) Ivankov, D. N.; Finkelstein, A. V. *J. Phys. Chem. B* **2010**, *114*, 7920–9.
- (7) Ivankov, D. N.; Finkelstein, A. V. *J. Phys. Chem. B* **2010**, *114*, 7930–4.
- (8) Turoverov, K. K.; Kuznetsova, I. M.; Uversky, V. N. *Prog. Biophys. Mol. Biol.* **2010**, *102*, 73–84.
- (9) Dunker, A. K.; Cortese, M. S.; Romero, P.; Iakoucheva, L. M.; Uversky, V. N. *FEBS J.* **2005**, *272*, 5129–48.
- (10) Uversky, V. N.; Oldfield, C. J.; Dunker, A. K. *Annu. Rev. Biophys.* **2008**, *37*, 215–46.
- (11) Tam, R.; Saier, M. H., Jr. *Microbiol. Rev.* **1993**, *57*, 320–46.
- (12) Dwyer, M. A.; Hellinga, H. W. *Curr. Opin. Struct. Biol.* **2004**, *14*, 495–504.
- (13) Vyas, N. K.; Vyas, M. N.; Quiocho, F. A. *J. Biol. Chem.* **1991**, *266*, 5226–37.
- (14) Chen, X.; Schauder; Potier, S. r,N.; Van Dorsselaer, A.; Pelczer, I. *Nature* **2002**, *415*, 545–9.
- (15) Vyas, N. K.; Vyas, M. N.; Quiocho, F. A. *Science* **1988**, *242*, 1290–5.
- (16) Borrok, M. J.; Kiessling, L. L.; Forest, K. T. *Protein Sci.* **2007**, *16*, 1032–41.
- (17) Dattelbaum, J. D.; Lakowicz, J. R. *Anal. Biochem.* **2001**, *291*, 89–95.
- (18) D'Auria, S.; Lakowicz, J. R. *Curr. Opin. Biotechnol.* **2001**, *12*, 99–104.
- (19) Shilton, B. H.; Flocco, M. M.; Nilsson, M.; Mowbray, S. L. *J. Mol. Biol.* **1996**, *264*, 350–63.
- (20) Tolosa, L.; Gryczynski, I.; Eichhorn, L. R.; Dattelbaum, J. D.; Castellano, F. N.; Rao, G.; Lakowicz, J. R. *Anal. Biochem.* **1999**, *267*, 114–20.
- (21) Oliver, N. S.; Toumazou, C.; Cass, A. E.; Johnston, D. G. *Diabet. Med.* **2009**, *26*, 197–210.
- (22) Pace, C. N. *Methods Enzymol.* **1986**, *131*, 266–80.
- (23) Dutta, S.; Burkhardt, K.; Young, J.; Swaminathan Matsuura Henrick, G. J.; T., K.; Nakamura, H.; Berman *Mol. Biotechnol.* **2009**, *42*, 1–13.
- (24) Turoverov, K. K.; Kuznetsova, I. M.; Zaitsev, V. N. *Biophys. Chem.* **1985**, *23*, 79–89.
- (25) Turoverov, K. K.; Kuznetsova, I. M. *J. Fluoresc.* **2003**, *13*, 41–57.
- (26) Kuznetsova, I. M.; Stepanenko, O. V.; Turoverov, K. K.; Staiano, M.; Scognamiglio, V.; Rossi, M.; D'Auria, S. *J. Proteome Res.* **2005**, *4*, 417–23.
- (27) Turoverov, K. K.; Bikhtashev, A. G.; Dorofeik, A. V.; Kuznetsova, I. M. *Tsitolgiia* **1998**, *40*, 806–17.
- (28) Kuznetsova, I. M.; Stepanenko, O. V.; Stepanenko, O. V.; Povarova, O. I.; Bikhtashev, A. G.; Verkhusha, V. V.; Shaylovsky, M. M.; Turoverov, K. K. *Biochemistry* **2002**, *41*, 13127–32.
- (29) Kuznetsova, I. M.; Turoverov, K. K.; Uversky, V. N. *J. Proteome Res.* **2004**, *3*, 485–94.
- (30) Stepanenko, O. V.; Kuznetsova, I. M.; Turoverov, K. K.; Huang, C.; Wang, C. C. *Biochemistry* **2004**, *43*, 5296–303.
- (31) Kuznetsova, I. M.; Stepanenko, O. V.; Turoverov, K. K.; Zhu, L.; Zhou, M.; Fink, A. L.; Uversky, V. N. *Biochim. Biophys. Acta* **2002**, *1596*, 138–55.
- (32) Nolting, B. *Protein Folding Kinetics. Biophysical Methods*; Springer-Verlag: Berlin-Heidelberg, 1999; p 191.
- (33) Marquardt, D. W. An algorithm for least-squares estimation of nonlinear parameters. *J. Soc. Ind. Appl. Math.* **1963**, *11*, 431–441.

- (34) Levitsky, D. I.; Rostkova, E. V.; Orlov, V. N.; Nikolaeva, O. P.; Moiseeva, L. N.; Teplova, M. V.; Gusev, N. B. *Eur. J. Biochem.* **2000**, *267*, 1869–77.
- (35) Kremneva, E.; Boussou; Nikolaeva, F. O.; Maytum, R.; Geeves, M. A.; Levitsky, D. I. *Biophys. J.* **2004**, *87*, 3922–33.
- (36) Levitsky, D. I. *The nature of biological systems as revealed by thermal methods*; Lorincz, D., Ed.; Kluwer Academic Publishers: Dordrecht Boston London, 2004; pp 127–158.
- (37) Privalov, P. L.; Potekhin, S. A. *Methods Enzymol.* **1986**, *131*, 4–51.
- (38) D'Auria, S.; Alfieri, F.; Staiano, M.; Pelella, F.; Rossi, M.; Iakowicz, J. R. *Biotechnol. Prog.* **2004**, *20*, 330–7.
- (39) D'Auria, S.; Ausili, A.; Marabotti, A.; Varriale, A.; Scognamiglio, V.; Staiano, M.; Bertoli, E.; Rossi, M.; Tanfani, F. *J. Biochem.* **2006**, *139*, 213–21.
- (40) Bushmarina, N. A.; Kuznetsova, I. M.; Biktashev, A. G.; Turoverov, K. K.; Uversky, V. N. *ChemBioChem* **2001**, *2*, 813–21.
- (41) Chen, Y.; Barkley, M. D. *Biochemistry* **1998**, *37*, 9976–82.
- (42) Piszczeck, G.; D'Auria, S.; Staiano, M.; Rossi, M.; Ginsburg, A. *Biochem. J.* **2004**, *381*, 97–103.
- (43) Hsin, J.; Arkhipov, A.; Yin, Y.; Stone, J. E.; Schulten, K. *Curr. Protoc. Bioinf.* **2008**, *S*, Unit 5.7.
- (44) Merritt, E. A.; Bacon, D. J. *Methods Enzymol.* **1977**, *277*, 505–524.